PERGAMON

Solid-State Electronics 46 (2002) 1085–1090

SOLID-STATE ELECTRONICS

www.elsevier.com/locate/sse

Study on dopant activation of phosphorous implanted polycrystalline silicon thin films by KrF excimer laser annealing

Chang-Ho Tseng, Ching-Wei Lin, Teh-Hung Teng, Ting-Kuo Chang, Huang-Chung Cheng *, A. Chin

Department of Electronics Engineering, Institute of Electronics, Building IV, National Chiao Tung University, 1001 Ta Hsueh Rd., Hsinchu 300, Taiwan, ROC

Received 19 August 2001; received in revised form 2 November 2001; accepted 4 December 2001

Abstract

The KrF excimer laser annealing of phosphorous implanted polycrystalline silicon (poly-Si) films had been investigated completely. Resistors were fabricated to measure sheet resistance of poly-Si film. The interference effect, heat absorption of capping oxide as well as transformation of poly-Si grain size during laser annealing were reported. Depending on the carrier concentrations, poly-Si exhibits different sheet resistance behavior when the excimer laser fluence is higher than the full-melt threshold fluence. The sheet resistance of poly-Si film has an abnormal increase from 5×10^4 to 4×10^6 $\Omega/\square$ when the excimer laser energy is higher than full-melt threshold energy.

Keywords: Excimer laser annealing; Dopant activation; Polycrystalline silicon thin film transistor; Active-matrix liquid crystal display

1. Introduction

Excimer laser annealing (ELA) has been studied extensively on high-performance polycrystalline silicon (poly-Si) thin-film transistors (TFTs) for active-matrix liquid crystal display (AMLCD) applications. These studies contain not only the crystallization of amorphous silicon (a-Si) thin film but also the dopant activation of source/drain regions. For a-Si thin film crystallization, many researches have been made completely. Those of them include effects of laser energy density, number of laser shot [1], annealing ambient, and laser beam shape [2]. For example, large grain size of poly-Si can be formed with special orientation, (1 1 1) orientation, by utilizing multi-shot process with exact laser energy of flat top excimer laser beam [1]. Such kind of grain structure could also be obtained from the irradiation of multi-scan with Gaussian shape excimer laser beam [2]. By using such large gain and excellent crystallinity of poly-Si thin film, the performance of poly-Si TFTs can be improved drastically.

Besides the crystallization of a-Si thin film, dopant activation is another application of ELA in low-temperature poly-Si TFTs fabrication. Low-sheet resistances (R_s) of source/drain regions and contacts are necessary for high-performance poly-Si TFTs fabricating on low-cost glass substrate. Comparing with conventional furnace annealing, laser annealing can efficiently activate the doping atoms in poly-Si film at room temperature. Several studies have been reported about the dopant activation by ELA process. Those of them include spin-on-dopant layer annealed by KrF excimer laser, gas immersion laser doping (GILD) process, and projection-GILD [3–5]. But the dopant activation of poly-Si thin film capped with silicon oxide by ELA is less studied. In addition, it is well known that the conducting behavior

* Corresponding author. Tel.: +886-3-5712121x54218; fax: +886-3-573-8343/8403.

E-mail address: hccheng@cc.nctu.edu.tw (H.-C. Cheng).

0038-1101/02/$ - see front matter
PII: S0038-1101(02)00046-1

Nomenclature

Symbols			
R_s	sheet resistance, Ω/□	J	current density, A/cm^2
E_a	activation energy, eV	A	area perpendicular to the flow, cm^2
E_d	energy density, mJ/cm^2	A^*	constant, A/cm^2 K^2
V_g	voltage across grain boundary, volt (V)	k	Boltzmann constant, J/K
V_a	applied voltage across resistor, volt (V)	T	temperature, K
I	current, ampere (A)	q	elementary charge, 1.60218×10^{-19} C

of poly-Si film varies with the poly-Si grain size especially when the carrier concentrations are closed to the bulk trap concentrations. However, study related with this topic was also seldom reported.

This paper investigates the dopant activation of phosphorus implanted poly-Si thin film by KrF ELA process. The effects of laser fluence, capping oxide thickness and the grain structure transformation after KrF ELA on the sheet resistance of poly-Si films were studied systematically.

2. Experimental

Resistors were used to investigate the sheet resistance of poly-Si film. The fabrication process of resistor is described as follows. a-Si film (100 nm) was deposited on the top of oxidized (0.5 μm) Si substrate by LPCVD at 550 °C. Sample A, B, C, and G were crystallized by solid phase crystallization (SPC) at 600 °C for 24 h in order to investigate the interference effect resulted from the capping oxide and excimer laser. Sample D, E, and F were crystallized by ELA with optimum annealing conditions at substrate temperature of 400 °C and capped with silicon oxide films of 76, 100, and 117.5 nm, respectively. Phosphorous ion implantation was performed at acceleration voltage of 40 keV and with dosage of 5×10^{15} cm^{-2} for all samples. After ion implantation, sample A, B, and C were capped with 76, 100, and 117.5 nm thick silicon oxide films by plasma enhanced chemical vapor deposition (PECVD) system. Scanning type KrF (248 nm) excimer laser with Gaussian shape of 1.8 mm width and 23 mm length were applied on these samples. The overlapping of two sequent shots and the laser frequency were fixed at 95% and 20 Hz. After ELA, the contact holes of resistors were formed. Al (500 nm) and Au/Al (200/500 nm) films were deposited on sample A, B, C, G and sample D, E, F respectively and patterned for metal pads. Al sintering process was carried out at 400 °C for 30 min in a N_2 gas ambient furnace. NH_3 plasma treatment was done at 300 °C for 3 h. Finally, HP4156 was used to characterize the resistance of resistors. In order to investigate resistor-to-resistor variation, 25 resistors were probed for each laser irradiation condition.

3. Results and discussion

The reflectance of poly-Si film capped with various thicknesses of silicon oxide film is shown in Fig. 1. On the other hand, inset shows the simulation result of poly-Si film reflectance which varies with the thickness of silicon oxide under KrF excimer laser (248 nm) irradiation. It is known as the interference effect. The measured reflectance is slightly lower than that of simulation. It should be caused from the light scattering by rough surface of poly-Si film [6].

According to the analysis from Fig. 1, the sheet resistances of sample A, B, and C have a good agreement with the interference effect as shown in Fig. 2. To reduce the sheet resistance of poly-Si thin film, sample C needs just the two-thirds amount of energy what sample A does. Differing from the results published in reference [1], the sheet resistance does not increase again due to

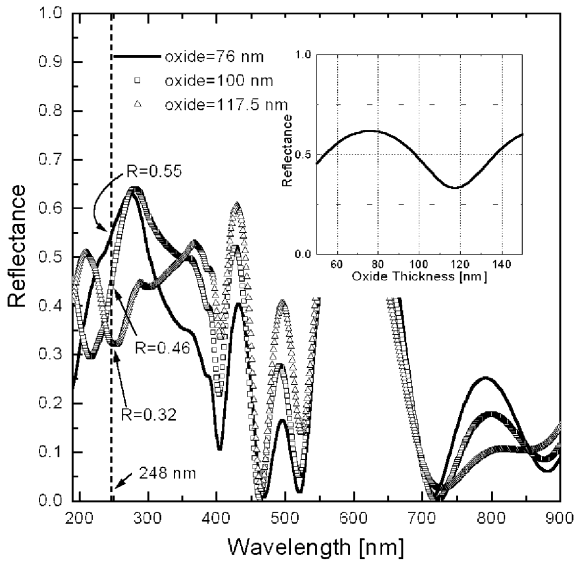

Fig. 1. Reflectance of poly silicon film capped with 76, 100, and 117.5 nm silicon oxide films. Inset shows the calculation result of poly-Si film reflectance varying with silicon oxide film thickness under KrF (248 nm) excimer laser exposing.

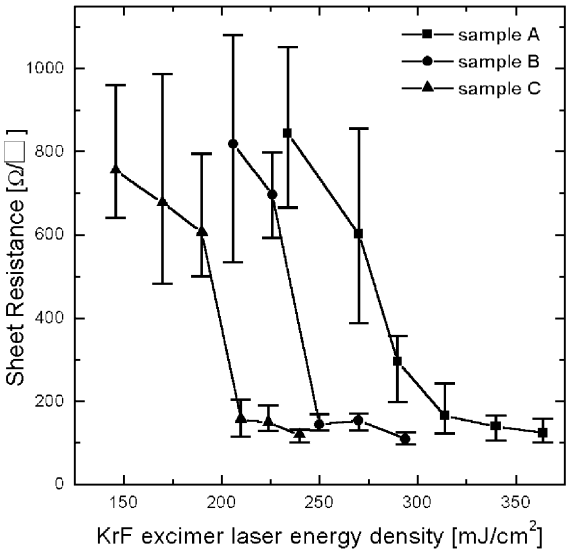

Fig. 2. Sheet resistance of poly-Si film in sample A, B, and C.

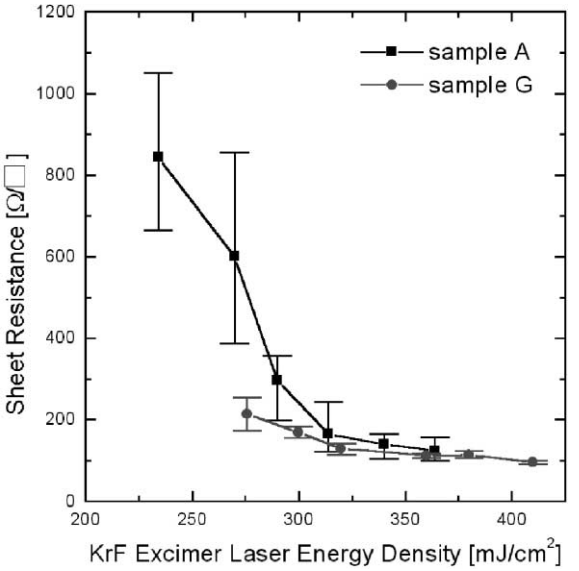

Fig. 3. Sheet resistance of poly-Si film in sample A (capped with 76 nm oxide film) and sample G (without capping oxide).

the amorphization of poly-Si film when high-laser fluence is applied. Due to the benefit of the scanning type laser beam with Gaussian shape, the silicon film can be retained in polycrystalline status during higher laser fluence annealing in our case. Consequently, the resistivity of poly-Si film does not increase again.

The sheet resistance of poly-Si film in sample G and A are shown in Fig. 3. From the optical analysis in Fig. 1, sample A absorbs the same or even higher laser energy than blank poly-Si film does under KrF ELA. However, the sheet resistance of poly-Si film in sample G is less than that of sample A. A reasonable explanation is that the capping oxide film acted as a heat absorber when poly-Si film was annealed with excimer laser. It decreased the activation ability of excimer laser particularly at low-laser fluence annealing. Although the silicon oxide consumes some heat from the molten poly-Si film, the sheet resistances of poly-Si thin film in sample A, B, and C actually meet the requirements of low-temperature poly-Si TFTs applications.

Figs. 4, 5, and 7 show the sheet resistance of sample D, E and F, respectively. After phosphorous ion implantation, the dopant concentrations of each sample are different due to the various thickness of capping oxide. Hall measurement was performed to take the carrier concentrations and Hall mobility of poly-Si film. Unfortunately, rough surface of poly-Si annealed by ELA, fluctuation of excimer laser energy as well as laser beam with Gaussian shape result in non-uniform grain structure of poly-Si film. They increase the difficulties to take exact data in Hall measurement. The approximate carrier concentrations of sample D, E, and F are 1.9×10^{20}, 2.2×10^{19}, and 2.5×10^{18} cm^{-3}, separately. It is well known that the carrier transport mechanism of

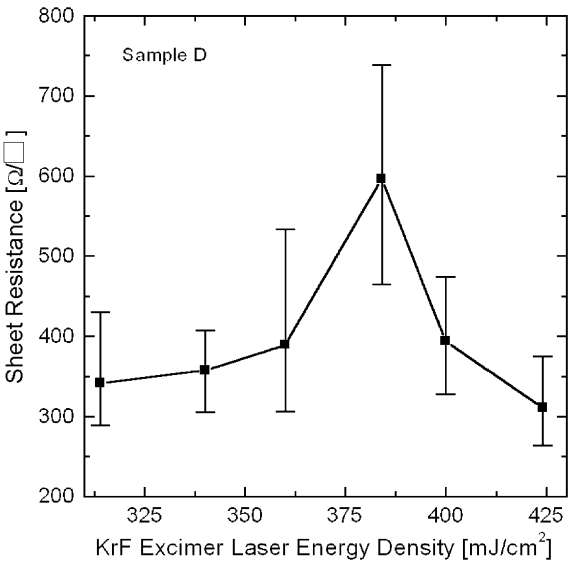

Fig. 4. Sheet resistance of poly-Si film in sample D.

poly-Si film greatly differs from that of c-Si [7]. At low-level dopant concentrations, the potential barrier resulted from the charges around the grain boundary is low, and depletion regions of grain boundary will be through the entire grain. Carriers can easily transport across the grain boundary by thermionic emission. As the dopant concentration increases, more carriers are trapped at the grain boundary; the height of potential barrier of the grain boundary increases and the depletion region within the grain does not change until all

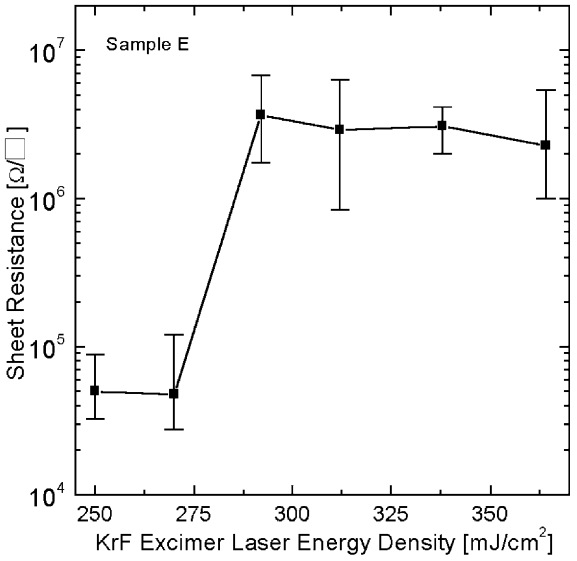

Fig. 5. Sheet resistance of poly-Si film in sample E.

traps are charged entirely. Carriers here are difficult to pass the potential barriers of grain boundaries. At high-dopant concentrations, all traps are charged and the added carriers, which are not trapped, cause the neutral regions within the grains. From the charge neutrality, the width of depletion regions decrease with increasing dopant concentration and so does the potential barrier heights. Carriers can transport across the grain boundaries easily by thermionic emission or even by tunneling.

The thickness of capping oxide of sample D is 76 nm. From the analysis of ion implantation simulation, we find that almost half amount of phosphorous ions pass through the oxide layer and stop in the poly-Si film. A high-carrier concentration of 1.9×10^{20} cm^{-3} suppresses the potential barrier of grain boundary and results in low-sheet resistance of sample D, as shown in Fig. 4. We also observe a peak around the laser energy density of 384 mJ/cm^2. This energy density is similar with the optimum crystallization energy of a-Si thin film with 100 nm thickness at room temperature. In addition, the poly-Si films of sample D, E, and F prepared by ELA with optimum laser energy at 400 °C substrate temperature have average grain size about 600 nm, which is examined by SEM. The grain size of poly-Si film under room temperature laser annealing will not reduce until that the laser fluence is higher than full-melt threshold (FMT) fluence. The average grain size decreases to about 150 nm after room temperature laser annealing with laser energy which is higher than FMT fluence. So the peak in Fig. 4 could be realized as the grain size shrinkage, and the decrease of sheet resistance at higher laser energy should be the increase of poly-Si crystallinity.

The sheet resistance of sample E exhibits an abnormal increase from 5×10^4 to 4×10^6 Ω/□ around the laser energy density of 290 mJ/cm^2 as shown in Fig. 5. From the analysis of Hall measurement, the approximate carrier concentration of sample E is 2.2×10^{19} cm^{-3}. However, the Hall mobility of poly-Si film decreases from 29 to 8 cm^2/V s when increasing laser energy. Besides the increase of grain boundaries, the increase of grain boundary potential barrier height should be the other reason resulting in abnormal increase of sheet resistance of poly-Si film in sample E. In order to clarify this assumption, the *I–V* characteristics of poly-Si film resistors irradiated with laser energy density of 250 and 336 mJ/cm^2 were measured over a range of temperatures.

Assuming the potential barriers at each grain boundary of poly-Si film are too wide for appreciable tunneling, the predominant transport mechanism is thermionic emission of majority carriers over the barriers. We suppose the applied voltage V_a, which is across the contacts of resistor, is dropped equally across the depletion zones at each of the grain boundaries and the voltage divides equally on both sides of each grain boundary. Then the voltage drop, V_g, across an individual grain boundary is

$$V_g = \frac{V_a}{N} \tag{1}$$

where N is equal to the number of grain boundaries between the contacts.

By considering thermionic emission in the two directions, forward and reverse current, the net current density can be found [8].

$$J = J_F - J_R = A^* T^2 \exp\left(\frac{-qV_B}{kT}\right)\left[\exp\left(\frac{qV_g}{2kT}\right) - \exp\left(\frac{-qV_g}{2kT}\right)\right] \tag{2}$$

or

$$I = AJ = 2K \sinh\left(\frac{qV_a}{2kTN}\right) \tag{3}$$

where V_B is the grain boundary barrier height at zero bias, A is the area perpendicular to the flow and

$$K = AA^* T^2 \exp\left(\frac{-qV_B}{kT}\right) \tag{4}$$

which were derived from Eqs. (2), and (3).

The *I–V* characteristics of poly-Si film irradiated with laser energy density of 250 and 336 mJ/cm^2 at various substrate temperatures are shown in Fig. 6. Empty scatter symbol indicates the measured results and solid line shows the fitted *I–V* curves of poly-Si films according to Eq. (3). Actually, the fitted *I–V* curves have a

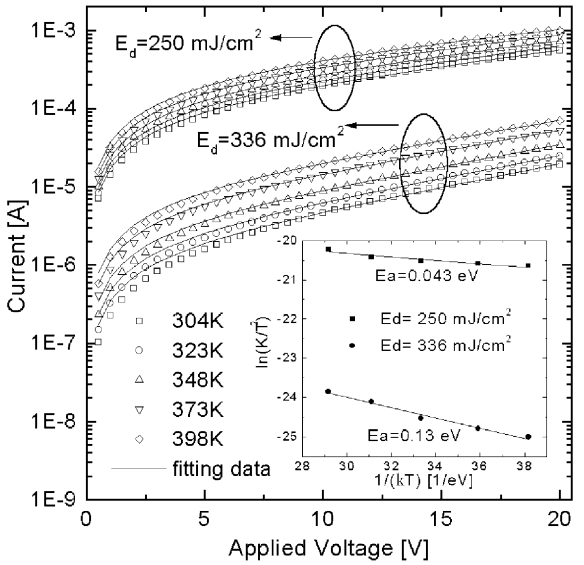

Fig. 6. Fitted and measured I–V characteristics of resistors in sample E over a range of temperature. Inset shows the fitting of grain boundary potential barrier height.

good agreement with measured ones. The value of K can be extracted from each one of the curves. The inset in Fig. 6 shows the plot of $\ln(K/T^2)$ vs. $1/kT$. Again, the potential barrier height of grain boundary can be extracted depending on Eq. (4). The potential barrier height of poly-Si film annealed with laser energy density of 336 mJ/cm^2 is 0.13 eV, which is larger than that of poly-Si film annealed with laser energy density of 250 mJ/cm^2 (0.04 eV). Therefore, the increase of grain boundary potential barrier height and shrinkage of grain size cause the abnormal increase in sheet resistance. In addition, the sheet resistance of poly-Si film in sample E is similar with that of poly-Si film in the lightly doped drain region of poly-Si TFT. These results can also be applied to the low-temperature lightly doped drain poly-Si TFTs fabrication.

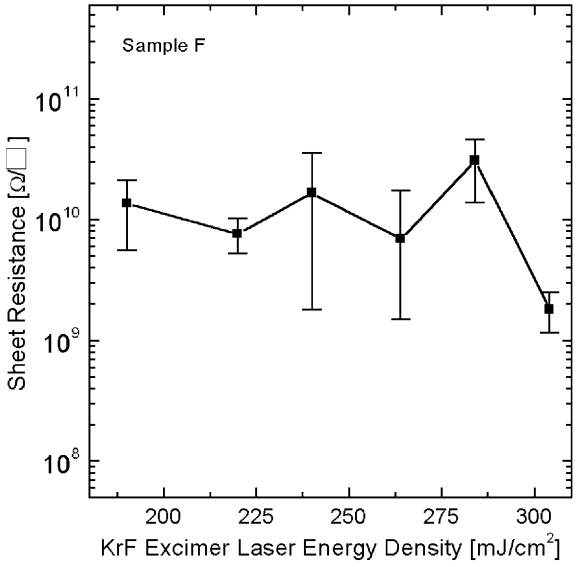

Fig. 7. Sheet resistance of poly-Si film in sample F.

The sheet resistance of sample F is not similar to that of sample E as shown in Fig. 7. Besides the deviation of sheet resistance near the FMT fluence, unobvious relationship between sheet resistance and laser energy density is observed, even if high-laser energy annealing decreases the grain size of poly-Si film. The approximate carrier concentration of poly-Si film in sample F is as low as 2.5×10^{18} cm^{-3}. It results in high resistivity within poly-Si grain. Hence, we cannot obviously observe the transformation of sheet resistance depending on the excimer laser energy density.

4. Conclusions

Dopant activation experiments have been accomplished in phosphorus ion implanted poly-Si film by KrF ELA. The consequences point out that the poly-Si film capped with silicon oxide film will cause the interference effect during KrF ELA. And the sheet resistance of poly-Si film annealed with sufficient laser energy can meet the requirements of low-temperature poly-Si TFTs applications. Moreover, we also clarify the mechanism of abnormal increase of sheet resistance when the carrier concentration of poly-Si film approximates to 2.2×10^{19} cm^{-3}. The increase of potential barrier height from 0.043 to 0.13 eV and the shrinkage of poly-Si grain size from 600 to 150 nm result in the abnormal increase of sheet resistance.

Acknowledgements

The authors would like to acknowledge the financial support by the National Science Council, Taiwan, ROC, under the Contract NSC-89-2215-E-009-108 and technical aid by Semiconductor Research Center (SRC) and SPRAD LAB, National Chiao Tung University, Taiwan, ROC.

References

[1] Giust GK, Sigmon TW. High-performance thin-film transistors fabricated using excimer laser processing and grain engineering. IEEE Trans Electron Dev 1998;45(4):925–32.

[2] Aaron M, Apostolos TV, Raj S. A systematic study and optimization of parameters affecting grain size and surface roughnes in excimer laser annealed polysilicon thin films. J Appl Phys 1997;82(9):4303–9.

[3] Al-Nuaimy EA, Marshall JM. Excimer laser crystallization and doping of source and drain regions in high quality amorphous silicon thin film transistors. Appl Phys Lett 1996;69:3857–9.
[4] Weiner KH, Carey PG, McCarthy AM, Sigmon TW. An excimer-laser-based nanosecond thermal diffusion technique for ultra-shallow pn junction fabrication. Microelectron Eng 1993;20:107–30.
[5] Kramer KJ, Somit T, Isabella TL, John ED, Kenneth AW, Keith AB, Kurt HW. Resistless, area-selective ultrashallow P+/N junction fabrication using projection gas immersion laser doping. Appl Phys Lett 1996;68:2320–2.
[6] Chiang KL, Dell'Oca CJ, Schwettmann FN. Optical evaluation of polycrystalline silicon surface roughness. J Electrochem Soc 1979;126:2267–9.
[7] Ted Kamins. Polycrystalline silicon for integrated circuits and displays. 2nd ed. Dordrecht: Kluwer Academic; 1998.
[8] George JK, Richard SM. Conduction properties of lightly doped, polycrystalline silicon. Solid-State Electron 1978; 21:1045–51.